Short Communication

Antiviral evaluation of bioactive azo derivatives to treat endemic poultry viruses

Tehreem Tahir[1] Muhammad Ashfaq[*2] Mirza Imran Shahzad[*1] Rukhsana Tabassum[2]

Abstract

The present study focused on the synthesis, *In Ovo* antiviral evaluation and *In silico* study of most active antiviral compounds of the azo series. The synthesis of title compounds was done by the coupling reaction of diazonium salt solutions with active methylene (1,3-dioxolane and benzimidazole), to yield [(*E*)-1-(1,3-dioxolan-2-yl)-2-phenyldiazene] (**A1**), [(*E*)-1-(1,3-dioxolan-2-yl)-2-(4-methyl-phenyl)diazene] (**A2**), 2-[(*E*)-phenyldiazenyl]-1*H*-benzimidazole] (**A3**) , [(*E*)-1-(1,3-dioxolan-2-yl)-2-(4-ethylphenyl)diazene] (**A4**) and [(*E*)-1-(1,3-dioxolan-2-yl)-2-(2-methylphenyl)diazene] (**A5**). The structures of newly synthesized molecules were elucidated by spectroscopic techniques (EI-MS and FT-IR). *In Ovo* screening of compounds against avian influenza virus (AIV) H9N2 strain and Newcastle Disease virus (NDV) Lasota strain was done. The evaluation data suggested that azo compound (**A5**) exhibited the highest anti-AIV and anti-NDV activity (100% inhibition at 0.1 mg/100 µL) compared to the other azo compounds which showed less activity at given concentrations. Docking study further suggested that azo compound (**A5**) binds with the active site residues of viral proteins with good binding affinity (-6.9 and -8.0 kcal/mol) compared to the standard oseltamivir due to the substitution of -CH_3 group at ortho position on the phenyl ring. Hence, based on this examination, it was concluded that azo compound (**A5**) may act as a platform for designing more active antiviral agents.

Keywords: Avian Influenza, Newcastle Disease, Therapeutic potential, Antiviral agents, Active methylene

[1]*Department of Biochemistry & Biotechnology, Faculty of Science, The Islamia University of Bahawalpur, Bahawalpur 63100, Pakistan*

[2]*Department of Chemistry, Faculty of Science, The Islamia University of Bahawalpur, Bahawalpur 63100, Pakistan*

***Correspondence**: mirza.imran@iub.edu.pk, chashfaqiub@yahoo.com* (M. Ashfaq, M. I. Shahzad)

Received March 23, 2020.

Accepted July 20, 2020.

Introduction

Viruses of the *Orthomyxoviridae* and *Paramyxoviridae* families are highly contagious and epidemic in nature that cause respiratory infections in birds and mammals leading to health and socio-economic threats (Mahesar *et al*., 2010; Zaitsev *et al*., 2004). Generally, there are two major surface proteins, Hemagglutinin (HA) and Neuraminidase (NA) in orthomyxoviruses, while, the paramyxoviruses have a hemagglutinin-neuraminidase (HN) protein and a fusion (F) protein, which are responsible for providing the attachment and penetration of viruses into target cells, thus providing potential targets for structure-based drug design (Chintakrindi *et al*., 2012; Zaitsev *et al*., 2004). Currently, there are two ways of decreasing the effect of viral infections *i.e.* vaccination or antiviral drugs (Beltra *et al*., 2016; Shaw Stewart, 2016). However, there are limitations related to vaccines, as their development has been greatly hindered by the high mutability of the virus and its developing subtypes (Crennell *et al*., 2000; Ganar *et al*., 2014), for which it is nearly impossible to supply vaccines in adequate amounts while antiviral drugs can meet the needs of the pandemic disaster as stated by Spackman *et al*., (2014) . Currently, there are two classes of anti-influenza drugs, one which targets the M2 ion channel (Adamantanes) and secondly that inhibits neuraminidase (Oseltamivir and Zanamivir) for influenza A and influenza B infections (Hu *et al*.,2007; Jackson *et al*., 2011; Song *et al*., 2007; Yang *et al*., 2013). Neuraminidase inhibitors have greater potential as sensitive anti-influenza drugs over the adamantanes due to their activity, improved safety profile and highly conserved active pocket residues in most of the influenza viral strains (Ju *et al*., 2018; Rahn *et al*. 2015). Many studies have been established to explore the inhibitory activities of compounds derived from natural sources and synthetic drugs. Among them, plant derived neuraminidase inhibitors show less activity compared to synthetic drugs (Bantia *et al*., 2001; Ju *et al*., 2018; Lupini *et al*., 2009). Therefore, there is always a dire need for such novel synthetic antiviral agents, that are less compromised by rapid drug resistant viral strains, that are efficient and have minimal side effects as described by Stratton *et al*., (2015).

Azo dyes (-N=N-) are a class of compounds which have attracted fascinated attention over the past few years due to their widespread use as dyes and pigments and diverse biomedical applications mentioned by Abdallah, (2012). Tevyashova *et al*., (2011) explored antiviral, Khanmohammadi *et al*. ,(2014) studied antibacterial, Mahata *et al*., (2014) evaluated antifungal, Gouda *et al*,. (2016) found antitumor while Shridhar *et al*., (2016) stated the hypotensive, anti-inflammatory and antioxidant potential of aromatic azo derivatives. Specifically against viruses, Naicker *et al*., (2004) identified an azo compound as a lead inhibitor of HIV-1 , Farghaly *et al*., (2009) discovered some of the highly active anti-HCV arylazobenzosuberones compared to ribavirin. Moreover, a series of highly active aminoarylazo compounds was evaluated against a panel of RNA viruses described by Tonelli *et al*., (2009).

To our knowledge, no study has been conducted to evaluate the bioactive potential of azo compounds against avian influenza virus (orthomyxovirus) and Newcastle Disease virus (paramyxovirus). Therefore, based on such evidence, a series of azo derivatives [(*E*)-1-(1,3–dioxolan-2-yl)-2-phenyldiazene] (**A1**), [(*E*)-1-(1,3–dioxolan-2-yl)-2-(4-methylphenyl)diazene] (**A2**), 2-[(*E*)-phenyldiazenyl]-1*H*-benzimidazole] (**A3**) , [(*E*)-1-(1,3–dioxolan-2-yl)-2-(4-ethyl-phenyl)diazene] (**A4**) and [(*E*)-1-(1,3–dioxolan-2-yl)-2-(2-methylphenyl) diazene] (**A5**) were synthesized by a coupling reaction of diazonium salt solutions with active methylene (1,3-dioxolane and benzimidazole). Structural determination/characterization was done by Mass and FT-IR spectroscopic analysis. The efficacy of synthesized compounds was assayed by *In Ovo* antiviral (NDV and AIV) activities and binding interaction was analyzed through molecular docking studies.

Materials and Methods

Chemistry: All solvents and chemicals were of analytical grade and purchased from Sigma-Aldrich and Merck. Melting points were adjusted using a calibrated thermometer by digital melting point apparatus (SMA10 of Stuart Scientific Bibby Sterilin Ltd., UK) and stated in degrees centigrade (°C). Pre-coated silica TLC plates (60F254 Merck Ltd., Japan) for determining purification, a magnetic stirrer (VELP Scientific England) for stirring and micropipettes (ZX58143 and ZX57677) for the TLC solvent system were used. The EI-MS spectra were elucidated by Finnigan MAT-12 spectrometer and expressed in m/z (%). The FTIR spectra were recorded with Bruker IR Tensor 27 (M15E-PS/09) by ATR sampling technique at a range of 4000-600 cm^{-1}.

[(*E*)-1-(1,3–dioxolan-2-yl)-2-phenyldiazene] (**A1**)

Sodium nitrite (1.73 g, 25 mmol) was mixed with aniline (2 g, 25 mmol) at 0 °C with continuous stirring for 20 minutes, then a few drops of 2M HCl was added and the reaction mixture was constantly stirred for 3 h until a yellow colored benzene diazonium salt was obtained which was neutralized with 1M Na_2CO_3. After that, 25 mM active methylene reagent (1,3-dioxolane) was added drop-wise in benzene diazonium chloride solution with constant stirring for 3-4 h until the final product of benzene diazonium azo compound (**A1**) was obtained. The final product was washed with distilled water and re-crystallized in 30 % methanol solution. Dark brown; yield: 65 %; m.p.: 100 ^{o}C; Solubility: MeOH, EtOH; R_f: 0.56; Mol. formula: $C_9H_{10}N_2O_2$; Mol. mass: 178 g/mol; MS (m/z): $[C_9H_{10}N_2O_2]^+$ M^+ 178 (9 %), $[C_6H_5N_2]^+$ 105 (65 %), $[C_3H_5O_2]^+$ 73 (14 %). $[C_6H_5N]^+$ 91 (30 %), $[C_6H_5]^+$ 77 (99 %), $[C_5H_5]^+$ 65 (27 %), $[C_4H_3]^+$ 51 (64 %); IR (cm^{-1}), 3000 (C-H), 1409 (N=N), 1183 (C-N), 1100 (C-O).

[(*E*)-1-(1,3–dioxolan-2-yl)-2-(4-methylphenyl)diazene] (**A2**)

Sodium nitrite (1.73 g, 25 mmol) was mixed with 4-methyl aniline (2 g, 25 mmol) at 0 °C with continuous

stirring for 20 minutes, then a few drops of 2M HCl was added and the reaction mixture was constantly stirred for 3 h until a yellow colored benzene diazonium salt was obtained which was neutralized with 1M Na_2CO_3. After that, 25 mM active methylene reagent (1,3-dioxolane) was added drop-wise in benzene diazonium chloride solution with constant stirring for 3-4 h until the final product of benzene diazonium azo compound (**A2**) was obtained. The final product was washed with distilled water and re-crystallized in 30 % methanol solution. Brown; yield: 72 %; m.p.: 121 ^oC; Solubility: MeOH, EtOH; R_f: 0.62; Mol. formula: $C_{10}H_{12}N_2O_2$; Mol. mass: 192 g/mol; MS (m/z): $[C_{10}H_{12}N_2O_2]^+$ M^+ 192 (5 %), $[C_7H_7N_2]^+$ 119 (39 %), $[C_3H_5O_2]^+$ 73 (29 %), $[C_7H_7]^+$ 91 (99 %), $[C_6H_5]^+$ 77 (38 %), $[C_5H_5]^+$ 65 (64 %), $[C_4H_3]^+$ 51 (29 %); IR (cm^{-1}), 3000 (C-H), 1440 (N=N), 1188 (C-N), 1050 (C-O).

2-[(*E*)-phenyldiazenyl]-1*H*-benzimidazole] (**A3**)

Sodium nitrite (1.73 g, 25 mmol) was mixed with aniline (2 g, 25 mmol) at 0 °C with continuous stirring for 20 minutes, then a few drops of 2M HCl was added and the reaction mixture was constantly stirred for 3 h until a yellow colored benzene diazonium salt was obtained which was neutralized with 1M Na_2CO_3. After that, 25 mM active methylene reagent (benzimidazole) was added drop-wise in benzene diazonium chloride solution with constant stirring for 3-4 h until the final product of benzene diazonium azo compound (**A3**) was obtained. The final product was washed with distilled water and re-crystallized in 30 % methanol solution. Light green; yield: 70 %; m.p.: 186 ^oC; Solubility: MeOH, EtOH; R_f: 0.57; Mol. formula: $C_{13}H_{10}N_4$; Mol. mass: 222 g/mol; MS (m/z): $[C_{13}H_{10}N_4]^+$ M^+ 222 (10 %), $[C_6H_5N_2]^+$ 105 (55 %), $[C_7H_5N_2]^+$ 117 (6 %), $[C_6H_5N]^+$ 91 (5 %), $[C_6H_5]^+$ 77 (98 %), $[C_5H_5]^+$ 65 (39 %), $[C_4H_3]^+$ 51 (62 %); IR (cm^{-1}), 3398 (N-H), 3028 (C-H), 1502 (N=N), 1180 (C-N).

[(*E*)-1-(1,3–dioxolan-2-yl)-2-(4-ethylphenyl)diazene] (**A4**)

Sodium nitrite (1.73 g, 25 mmol) was mixed with 4-ethyl aniline (2 g, 25 mmol) at 0 °C with continuous stirring for 20 minutes, then a few drops of 2M HCl was added and the reaction mixture was constantly stirred for 3 h until a yellow colored benzene diazonium salt was obtained which was neutralized with 1M Na_2CO_3. After that, 25 mM active methylene reagent (1,3-dioxolane) was added drop-wise in benzene diazonium chloride solution with constant stirring for 3-4 h until the final product of benzene diazonium azo compound (**A4**) was obtained. The final product was washed with distilled water and re-crystallized in 30 % methanol solution. Light brown; yield: 68 %; m.p.: 92 ^oC; Solubility: MeOH, EtOH; R_f: 0.64; Mol. formula: $C_{11}H_{14}N_2O_2$; Mol. mass: 206 g/mol; MS (m/z): $[C_{11}H_{14}N_2O_2]^+$ M^+ 206 (6 %), $[C_8H_9N_2]^+$ 133 (60 %), $[C_3H_5O_2]^+$ 73 (10 %), $[C_8H_9]^+$ 105 (98 %), $[C_6H_5]^+$ 77 (40 %), $[C_5H_5]^+$ 65 (73 %), $[C_4H_3]^+$ 51 (27 %); IR (cm^{-1}), 2959 (C-H), 1442 (N=N), 1191 (C-N), 1055 (C-O).

[(*E*)-1-(1,3–dioxolan-2-yl)-2-(2-methylphenyl)diazene] (**A5**)

Sodium nitrite (1.73 g, 25 mmol) was mixed with 2-methyl aniline (2 g, 25 mmol) at 0 °C with continuous stirring for 20 minutes, then a few drops of 2M HCl was added and the reaction mixture was constantly stirred for 3 h until a yellow colored benzene diazonium salt was obtained which was neutralized with 1M Na_2CO_3. After that, 25 mM active methylene reagent (1,3-dioxolane) was added drop-wise in benzene diazonium chloride solution with constant stirring for 3-4 h until the final product of benzene diazonium azo compound (**A5**) was obtained. The final product was washed with distilled water and re-crystallized in 30 % methanol solution. Pinkish; yield: 80 %; m.p.: 45 ^oC; Solubility: MeOH, EtOH; R_f: 0.55; Mol. formula: $C_{10}H_{12}N_2O_2$; Mol. mass: 192 g/mol; MS (m/z): $[C_{10}H_{12}N_2O_2]^+$ M^+ 192 (6 %), $[C_7H_7N_2]^+$ 119 (39 %), $[C_3H_5O_2]^+$ 73 (28 %), $[C_7H_7]^+$ 91 (99 %), $[C_6H_5]^+$ 77 (38 %), $[C_5H_5]^+$ 65 (64 %), $[C_4H_3]^+$ 51 (29 %); IR (cm^{-1}), 3000 (C-H), 1502 (N=N), 1104 (C-N), 1050 (C-O).

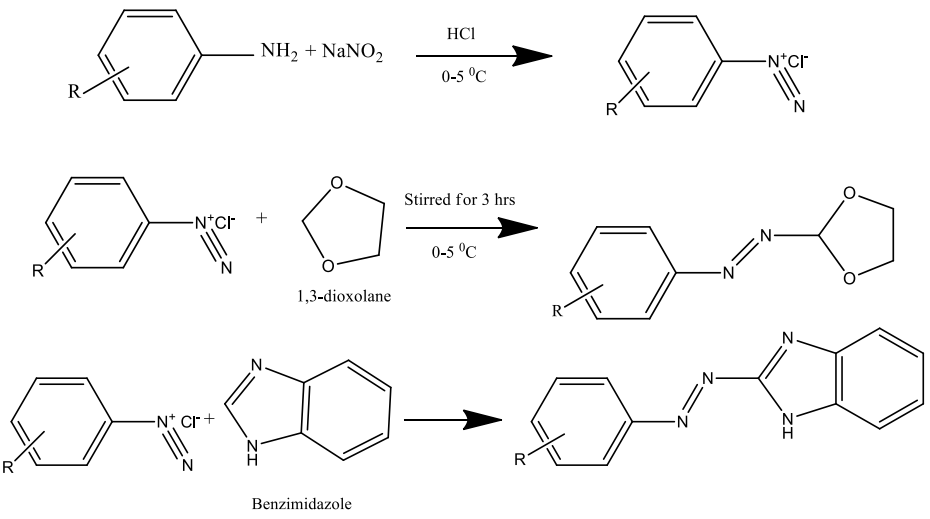

Figure 1 Synthesis scheme of azo compounds (**A1**-**A5**).

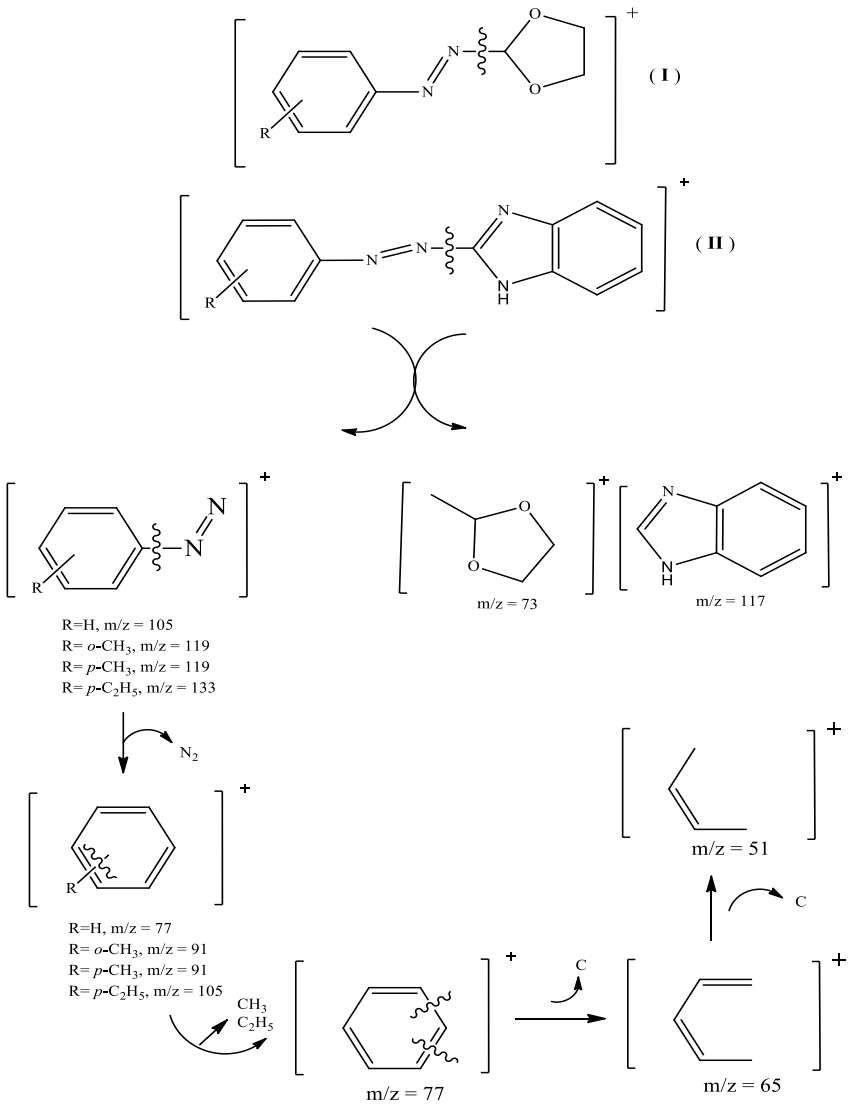

Figure 2 General fragmentation pattern of azo compounds (**A1**-**A5**).

Cultivation of Viruses: Specific pathogen free (SPF) embryonated chicken eggs were obtained from the Government Poultry Farm, Bahawalpur. Lasota strain of NDV, AIV H9N2 strain vaccine (Gallimune Flu H9 M.E from Merial Laboratories Italy), was obtained from the University College of Veterinary and Animal Sciences, The Islamia University of Bahawalpur. The respective viral strains were inoculated into 7-to -11 days old embryonated eggs through the chorio-allantoic route and incubated at 37 °C. The eggs were harvested 48 h post inoculation (PI), viral titer was assessed as per the method of Sekhar *et al.,* (2014) and the viral stocks were stored at -40 °C.

Antiviral Assay: *In Ovo* antiviral testing of the title compounds was carried out in developing chick embryos. Briefly, nine-day old SPF embryonated chicken eggs were labeled according to the testing compounds. The eggs were sterilized with 70 % alcohol and were placed in a micro safety cabinet, where they were drilled with sterile pins and compound/virus mixture was inoculated via the allantoic route. The compound/virus mixture was prepared by mixing 0.1 mL of virus in 0.1 mL of 1 mg/mL compound in DMSO (stock). Virus dissolved in saline solution was used as a negative control. Allantoic fluids were harvested 48 h PI, for Hemagglutination test to quantify the viruses.

Hemagglutination (HA) Test: Fresh chicken blood was taken in Alsever's solution and centrifuged at 4000 rpm for 15 mins. The supernatant was discarded and RBCs were washed with 0.10 M PBS (pH 7.2). This step was repeated until a clear supernatant was obtained. The 1 % suspension of RBCs was prepared by mixing 10 µL of packed cells in 1 mL of 0.1 M PBS. Later, the standard HA test was performed as described by Hirst (1942).

Molecular Docking: The three-dimensional X-ray crystallographic structures of PDB IDs 1NN2 and 1USX were downloaded from the RCSB Protein Data Bank (http://www.rcsb.org/pdb/home/home.do). The docking simulation was performed by virtual screening tool PyRx with VINA wizard and PyMOL (0.8) was used for structural representation. Protein preparation was done by the removal of water, the addition of polar hydrogen and kollman charges, processed to the respective. pdbqt file formats. Similarly, ligand file was prepared by the addition of polar hydrogen and gasteiger charges were given and

there was no further change on the ligand torsion tree, accessed to. pdbqt file formats. A grid box was prepared with parameters as follows: grid box center coordinate: 87.70, -87.29, -65.29; box size: 61, 62, 80; grid point spacing: 0.375 Å. The grid box was adjusted so that the ligand moved freely in search space within the binding pocket residues. After the optimized conditions were set, compound (**5**) and oseltamivir were docked with respective viral proteins (1NN2 and 1USX) and the best binding conformation with minimum binding energy (kcal/mol) was used for visualization using PyMOL.

Results and Discussion

Chemistry: The MS spectra of azo compounds (**A1-A5**) showed that the fragments were easily patronized with prominent molecular ion peaks (M^+) at m/z 178.0, 192.0, 222.1, 206.0 and 192.0 respectively. Major fragments were observed at m/z 133, 119, 105, 91, 77, 73, 65 and 51. The fragmentation mostly resulted in phenylethyl, benzyl and phenyl radicals and ended in $[C_4H_3]^+$ methylium ion with m/z 51. The general pattern of fragmentation is given in Figure **2**. Similarly, the detailed interpretation of IR spectra revealed the formation of azo compounds (**A1-A5**) as the appearance of aromatic secondary amine (N-H) peaked at ~3450 cm^{-1}, the presence of aromatic C-H stretch (3200-2800 cm^{-1}), strong azo -N=N- stretch (1630-1575 cm^{-1}), secondary amine C-N stretch (1190-1130 cm^{-1}) and a primary C-O stretch at ~1050 cm^{-1}. The spectroscopic data was found to be consistent with the literature stated by Coates, (2006).

Biological Study: All eggs were inoculated with a virus control and the results of Hemagglutination (HA) test in the case of anti-NDV potential of azo compounds (Fig. **3**) revealed that azo compound (**A5**) actively inhibited viral propagation (100% at 0.1 mg/ 100 µL) while compounds (**A3**) and (**A4**) inhibited 50% of viral growth at given concentrations. However, the tested compounds (**A1**) and (**A2**) were found inactive in this regard. Similarly, in the case of anti-AIV activity of azo compounds, only compounds (**A3**) (40% at 0.1 mg/ 100 µL) and (**A5**) (100% at 0.1 mg/ 100 µL) were able to kill the viral population. It was found that compound (**A5**) has the maximum potential to inhibit both viruses *i.e.* NDV and AIV. With the decrement of concentration *i.e.* 0.01 mg/ 100 µL, compound (**5**) showed 50% activity against both viruses (**Table 1**). Therefore, the initial screening data suggested further analysis of most potent compounds (**A5**) by docking simulation against viral proteins of NDV and AIV (H9N2).

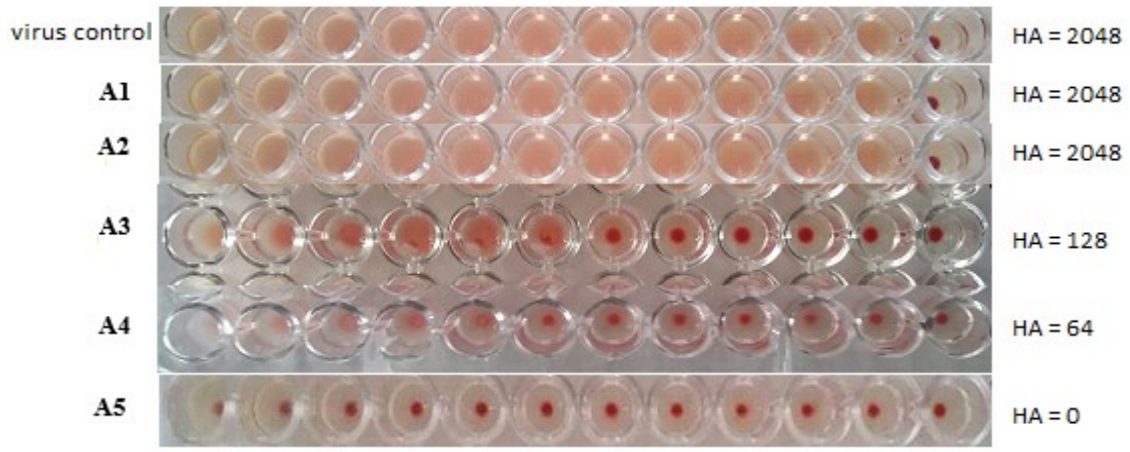

Figure 3 HA test results of azo compounds (**A1-A5**) against NDV at 0.1 mg/100 µL.

Docking Study: To understand the interaction, blind docking studies of the tested compound (**A5**) to the crystal structures of N2-subtype of avian influenza virus (PDB code: 1NN2) and hemagglutinin-neuraminidase dimer of newcastle disease virus (PDB code: 1USX), were conducted and the generated docked complexes were examined on the basis of minimum energy values (kcal/mol), bonding interactions such as hydrogen and hydrophobic bonds respectively. Oseltamivir was used as a comparative binding interaction analysis by *McClellan et al., (2001).* The best conformational docked pose of azo (**A5**)-1NN2 with binding affinity -6.9 kcal/mol is shown in Fig. **4**, which shows that both nitrogen atoms of azo moiety and oxygen atoms from 1,3-dioxolane formed strong hydrogen bonds with Arg283, Asp355 and Asn356 with bond lengths of 2.96, 3.77 and 3.59 Å, respectively. Similarly, hydrophobic interactions were seen between the methyl-phenyl ring of azo (**A5**) and Ser88, Pro285, Pro282, Arg283 and Asn356 with bond lengths 3.27, 3.32, 3.21, 3.87 and 3.27 Å. However, a π-π interaction was observed between carbon atoms of 1,3-dioxolane ring and Tyr283 with bond length 3.29 Å. In case of oseltamivir-1NN2 docked complex (Fig. **4**), hydrogen bonding was observed between nitrogen atoms of the acetamido ring and Val127 with a bond length of 3.27 Å with binding affinity -6.5 kcal/mol, while, hydrophobic interactions were seen among the carbon atoms of the oxy-cyclohexene ring and residues Cys124, Cys129 and Val412 with bond lengths 3.89, 3.54 and 3.64 Å respectively.

The docking results of azo compound (**A5**)-1USX (Fig. **5**) suggested that hydrogen bonding exists between nitrogen atoms of azo moiety and Asn161 and

Pro164 with bond lengths 3.13 and 3.02 Å, however, the nitrogen and oxygen atoms of 1,3-dioxolane showed weak interactions with Pro164 and a π-π bond was observed between carbon atoms of 1,3-dioxolane and Tyr205 and Ser226 with binding affinity -8.0 kcal/mol. Similarly, the docked complex of oseltamivir-1USX (free binding energy -7.5 kcal/mol) shows (Fig. **5**) that nitrogen atoms of 4-acetamido and 5-amino rings were involved in hydrogen bonding with residues Ileu136 and Gly137 with bond lengths 3.13 and 2.7 Å, whereas carboxylate moiety made hydrophobic interaction with Ala182 and the oxy-cyclohexene ring made other interactions with residues Ala182, Lys138 and Thr406. Studies have revealed that hydrogen bonds play an important role in stabilizing and strengthening the docked complexes (Bikadi *et al.*, 2007; McDonald *et al.*, 1994). It is therefore inferred that the substitution of -CH_3 group at ortho position gives the perfect geometry to the small structural molecule of azo compound (**A5**) with relatively stable docked complex and maximum antiviral effect.

In conclusion, the azo compounds were successfully synthesized under reproducible conditions and were obtained in good yields. It can be inferred from the results of the antiviral activity and computational studies that the azo compound (**A5**) can be further analyzed against other influenza viral strains and can serve as a structural template in the design of novel antiviral agents since there are fewer synthetic antiviral drugs available commercially.

Conflict of Interest: The authors declare no conflict of interest.

Table 1 Antiviral potential of azo compounds. HA titer corresponds to the viral growth

Compounds	Concentration (mg/ 100 µL)	NDV		AIV (H9N2)	
		HA titer	% inhibition	HA titer	% inhibition
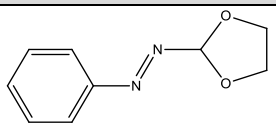 **A1**	0.1	2048	0	2048	0
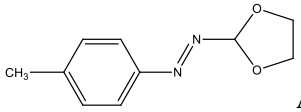 **A2**	0.1	2048	0	2048	0
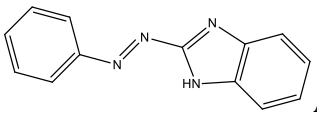 **A3**	0.1	128	50	512	40
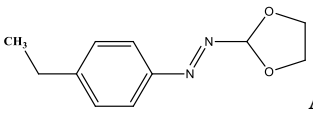 **A4**	0.1	64	50	2048	0
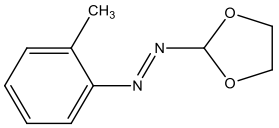 **A5**	0.1 0.01	0 128	100 50	0 64	100 50

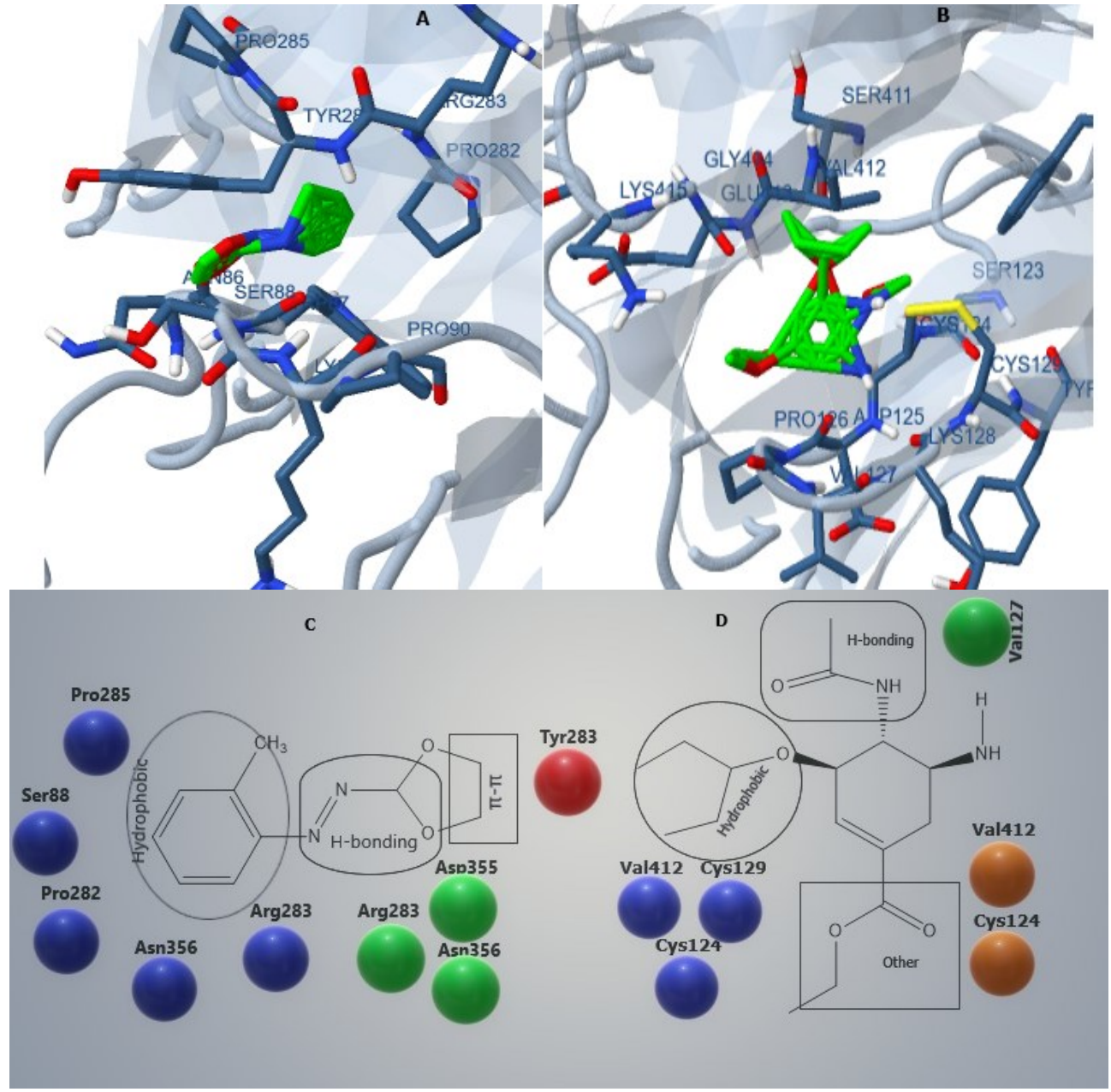

Figure 4 **(A).** Structural representation of docking complex of azo compound (**A5**) (sticks with carbon atoms shown as: green, nitrogen: blue and oxygen: red) with interacting side chain residues of neuraminidase (PDB code: 1NN2) shown as dark blue cylinders. **(B).** key residues in contact with oseltamivir (green sticks). **(C).** Structural interactions exhibited by azo (**A5**). **(D)**. Interaction shown by components of oseltamivir.

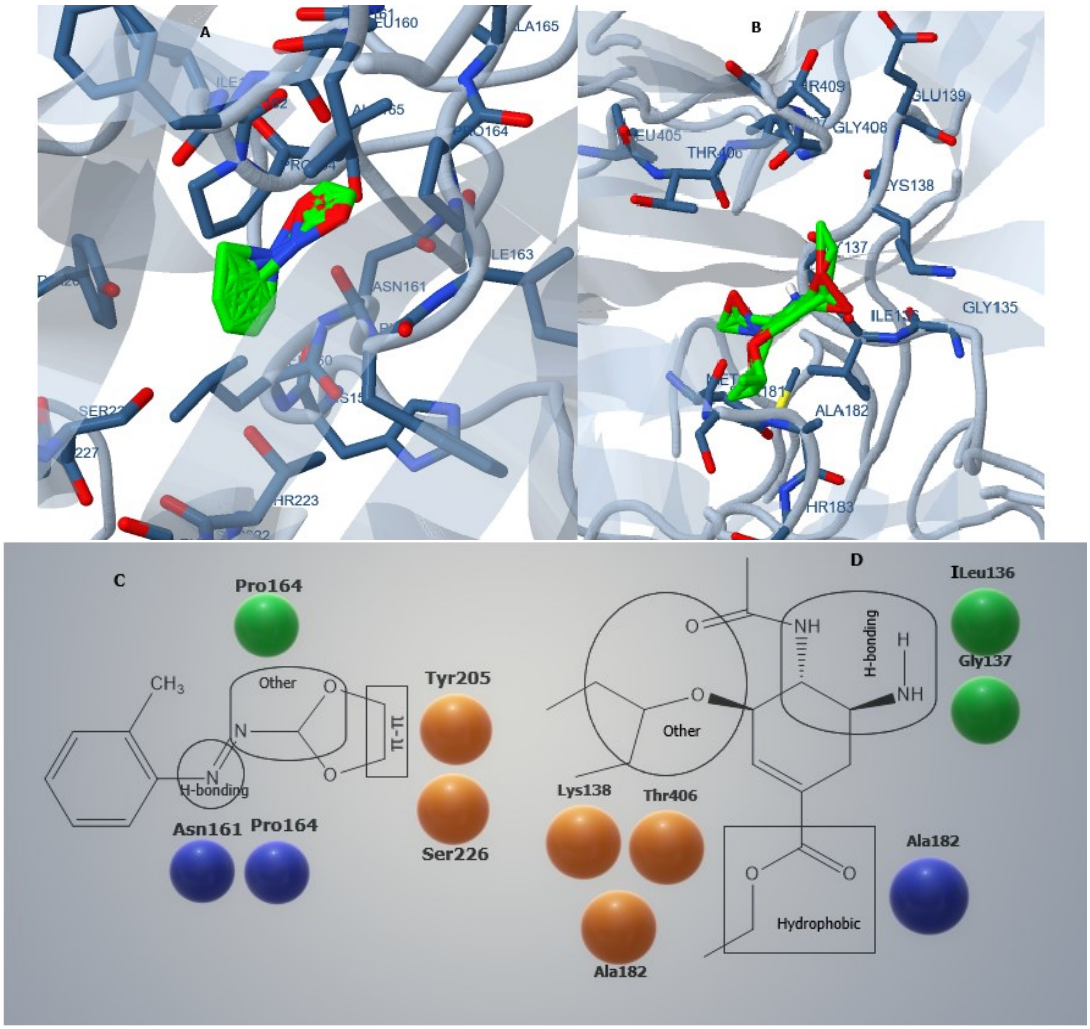

Figure 5 **(A)**. Docking complex of HN dimer of Newcastle Disease virus (PDB code: 1USX) with best pose of azo compound (**A5**) against target residues. **(B)**. The closer view of binding pocket interaction with best conformation position of oseltamivir against target residues. **(C)**. key interactive components observed in **A5**-1USX complex. **(D).** structural features of oseltamivir docked with 1USX.

Acknowledgement

The authors are grateful to the Department of Chemistry, The Islamia University of Bahawalpur, Pakistan for co-operation and assistance throughout the project.

References

Abdallah SM 2012. Metal complexes of azo compounds derived from 4-acetamidophenol and substituted aniline. Arab J Chem. 5; 251-256.

Bantia S, Parker C, Ananth S, Horn L, Andries K, Chand P, Kotian P, Dehghani A, El-Kattan Y and Lin T 2001. Comparison of the anti-influenza virus activity of RWJ-270201 with those of oseltamivir and zanamivir. Antimicrob Agent Chemother. 45; 1162-1167.

Beltra J-Cand Decaluwe H 2016. Cytokines and persistent viral infections. Cytokine. 82; 4-15.

Bikadi Z, Demko, Land HE 2007. Functional and structural characterization of a protein based on analysis of its hydrogen bonding network by hydrogen bonding plot. Archiv Biochem Biophy. 461; 225-234.

Chintakrindi A, D'souza C and Kanyalkar M 2012. Rational development of neuraminidase inhibitor as a novel anti-flu drug. Mini Rev Med Chem. 12; 1273-1281.

Coates J 2006. Interpretation of infrared spectra, a practical approach. Encyclopedia of analytical chemistry: applications, theory and instrumentation. Wiley Online Library.

Crennell S, Takimoto T, Portner A and Taylor G 2000. Crystal structure of the multifunctional paramyxovirus hemagglutinin-neuraminidase. Nature Struct Mol Biol. 7; 1068.

Farghaly TA and Abdalla MM 2009. Synthesis, tautomerism, and antimicrobial, anti-HCV, anti-SSPE, antioxidant, and antitumor activities of arylazobenzosuberones. Bioorg Med Chem. 17; 8012-8019.

Ganar K, Das M, Sinha S and Kumar S 2014. Newcastle disease virus: Current status and our understanding. Virus Res. 184; 71-81.

Gouda MA, Eldien HF, Girges MM and Berghot MA 2016. Synthesis and antitumor evaluation of thiophene based azo dyes incorporating pyrazolone moiety. J Saudi Chem Soc. 20; 151-157.

Hirst GK 1942. The quantitative determination of influenza virus and antibodies by means of red cell agglutination. J Experiment Med. 75; 49-64.

Hu J, Asbury T, Achuthan S, Li C, Bertram R, Quine JR, Fu R and Cross TA 2007. Backbone structure of the amantadine-blocked trans-membrane domain M2 proton channel from influenza A virus. Biophy J. 92; 4335-4343.

Jackson RJ, Cooper KL, Tappenden P, Rees A, Simpson EL, Read, RC and Nicholson KG 2011. Oseltamivir, zanamivir and amantadine in the prevention of influenza: A systematic review. J Infect. 62; 14-25.

Ju H, Zhang J, Sun Z, Huang Z, Qi W, Huang B, Zhan P and Liu, X 2018. Discovery of C-1 modified oseltamivir derivatives as potent influenza neuraminidase inhibitors. Euro J. Med Chem. 146; 220-231.

Khanmohammadi H, Pass M, Rezaeian K and Talei G 2014. Solvatochromism, spectral properties and antimicrobial activities of new azo–azomethine dyes with N2S2O2 donor set of atoms. J Mol Struct. 1072; 232-237.

Lupini C, Cecchinato M, Scagliarini A, Graziani R and Catelli E 2009. In vitro antiviral activity of chestnut and quebracho woods extracts against avian reovirus and metapneumovirus. Res Vet Sci. 87; 482-487.

Mahata D, Mandal SM, Bharti R, Gupta VK, Mandal M, Nag A and Nando GB 2014. Self-assembled cardanol azo derivatives as antifungal agent with chitin-binding ability. Int J Bio Macromol. 69; 5-11.

Mahesar SA, Sherazi STH, Niaz A, Bhanger MI, uddin S and Rauf A 2010. Simultaneous assessment of zinc, cadmium, lead and copper in poultry feeds by differential pulse anodic stripping voltammetry. Food Chem Toxicol. 48; 2357-2360.

McClellan K and Perry, CM 2001. Oseltamivir. Drugs. 61; 263-283.

McDonald IK and Thornton JM 1994. Satisfying hydrogen bonding potential in proteins. J Mol Bio. 238; 777-793.

Naicker KP, Jiang S, Lu H, Ni J, Boyer-Chatenet L, Wang L-X and Debnath AK 2004. Synthesis and anti-HIV-1 activity of 4-[4-(4,6-bisphenylamino-[1,3,5]triazin-2-ylamino)-5-methoxy-2-methylphenylazo]-5-hydroxynaphthalene-2,7-disulfonic acid and its derivatives. Bioorg Med Chem. 12; 1215-1220.

Rahn J, Hoffmann D, Harder TC and Beer, M 2015. Vaccines against influenza A viruses in poultry and swine: Status and future developments. Vaccine. 33; 2414-2424.

Sekhar KC, Janardhan A, Kumar YN, Narasimha G, Raju CN and Ghosh S 2014. Amino acid esters substituted phosphorylated emtricitabine and didanosine derivatives as antiviral and anticancer agents. Appl Biochem Biotechnol. 173; 1303-1318.

Shaw Stewart PD 2016. Seasonality and selective trends in viral acute respiratory tract infections. Med Hypo. 86; 104-119.

Shridhar AH, Keshavayya J, Peethambar SK and Joy Hoskeri H 2016. Synthesis and biological activities of Bis alkyl 1,3,4-oxadiazole incorporated azo dye derivatives. Arab J Chem. 9, Supplement 2; S1643-S1648.

Song JM, Park KD, Lee KH, Byun YH, Park JH, Kim SH, Kim JH and Seong BL 2007. Biological evaluation of anti-influenza viral activity of semi-synthetic catechin derivatives. Antivir Res. 76; 178-185.

Spackman E and Pantin-Jackwood MJ 2014. Practical aspects of vaccination of poultry against avian influenza virus. The Vet J. 202; 408-415.

Stratton CF, Newman DJ and Tan DS 2015. Cheminformatic comparison of approved drugs from natural product versus synthetic origins. Bioorg Med Chem Lett. 25; 4802-4807.

Tevyashova AN, Shtil AA Olsufyeva EN, Luzikov YN, Reznikova MI, Dezhenkova LG, Isakova EB, Bukhman VM, Durandin NA, Vinogradov AM, Kuzmin VA and Preobrazhenskaya MN 2011. Modification of olivomycin A at the side chain of the aglycon yields the derivative with perspective antitumor characteristics. Bioorg Med Chem. 19; 7387-7393.

Tonelli M, Vazzana I, Tasso B, Boido V, Sparatore F, Fermeglia M, Paneni MS, Posocco P, Pricl S, Colla PL, Ibba C, Secci B, Collu G and Loddo R 2009. Antiviral and cytotoxic activities of aminoarylazo compounds and aryltriazene derivatives. Bioorg Med Chem. 17; 4425-4440.

Yang J, Li M, Shen X and Liu S 2013. Influenza A virus entry inhibitors targeting the hemagglutinin. Virus. 5; 352-373.

Zaitsev V, Von IM, Groves D, Kiefel M, Takimoto T, Portner A and Taylor G 2004. Second sialic acid binding site in Newcastle disease virus hemagglutinin-neuraminidase: implications for fusion. J Virol. 78; 3733-3741.